Advances in tuning band gap of graphene by potential doping using DFT: a review

I. Rahim[a], S. Azam[b,*], B. Gul[c], A. A. Khan[a], N. Yousaf[a], Z. Zada[d], M. Saqib[j],
F. Subhan[e], M. Ismail[k], A. Khan[a], G. Murtaza[d], A. Dahshan[f,g], S. S. Ahmad[h],
A. Kalsoom[i], M. Sheraz[e], H. H. Hegazy[f]
[a]*Department of Physics, University of Peshawar, Peshawar, Pakistan*
[b]*Faculty of Engineering and Applied Sciences, Department of Physics, RIPHAH
International University, I-14 Campus, Islamabad, Pakistan*
[c]*National University of Sciences and Technology (NUST), Islamabad, Pakistan*
[d]*Materials Modelling Lab, Department of Physics, Islamia College University,
Peshawar, Pakistan*
[e]*Department of Physics, Government Post Graduate College, Swabi, Pakistan*
[f]*Department of Physics - Faculty of Science - King Khalid University, P.O. Box
9004, Abha, Saudi Arabia.*
[g]*Department of Physics, Faculty of Science, Port Said University, Port Said,
Egypt.*
[h]*Department of Physics, University of Swabi, Pakistan*
[i]*Department of Physics, The Government Sadiq College Women University,
Bahawalpur, Pakistan*
[j]*Department of Electrical and Computer Engineering, COMSATS University
Islamabad, Abbottabad Campus, KPK, Pakistan*
[k]*Department of Chemistry, Women University Swabi, KPK, Pakistan*

Graphene: a sp^2 carbon system is a zero band gap semiconductor. In spite of having extraordinary properties, opening of band gap is the bottleneck in the path of graphene for becoming the heart of all modern electronics. Chemical doping can prove itself to be the fastest solution to this problem as it is one of the most informal approaches to induce band gap in pristine. Due to tiny nanostructures and dimensions of graphene, modelling and simulative study of graphene is more effective and confirmative than experimental results. In this study we have compared our results with the previous works, our simulation matches well with the previous works. The main concern is on the substitution and pair doping of BN, B and N open up an energy band gap up to (0.379eV) and (0.386eV). Co-doping of B-N create a band gap up to (0.712eV) and pair doping shows that 1BN(0.616eV), 2BN(0.386eV), 3BN pair create a sharp increase in band gap up to (1.457eV) when substitute on graphene, while the substitution doping and increased in the super cell models with the same doping concentration of silicon induced a band gap of 1.019eV, where Si doping on different super cell shows a band gap enhancement from 0.57eV at (6x6) model to 1.90eV at (5x5) model and change its nature from semimetal to semiconductor. The present review article focuses on the alteration of electronic and optical properties by adding different dopants on to the graphene sheets, using density functional theory (DFT) calculations. Doping can improve the electronic properties of graphene by producing a small band gap in it, resulting in the appropriateness of this interesting material for modern electronics. Different codes and approximations have been applied to tune the band structure of graphene that has been discussed in the article.

---

* Corresponding author: sikandar.azam@riphah.edu.pk

1. Introduction

One of the most fascinating discoveries since 2004 which has captured the undivided attention of scientist is that of 'one atom thick honey comb structure of graphene' [1]. It has been under intense scrutiny for its optoelectronic properties from the very first moment of its known existence [2-6]. While observing it as a two dimensional sheets, the analogous Bloch states of graphene are created for the most part by the carbon valence p_z orbital forming two π bands (cones). The other three carbon atoms form σ bonds via sp^2 hybridization, accountable for the structural permanence of graphene [7]. The invigorating properties such as high carrier mobility ($\sim$10,000 cm^2/V s) [1], quantum hall effect at room temperature [8-9], outstanding optical transparency ($\sim$97.7%) [10], large theoretical specific surface area (2630 m^2/g) [11], high Young's modulus ($\sim$1TPa) [12] and excellent thermal conductivity (TC) ($\sim$3000W/mK) [13] are endorsed to the only one of its kind structure of graphene. Furthermore, graphene is considered to be the building unit of all the other graphitic carbon allotropes of diverse dimensionality as illustrated in figure 1 [14]. All these properties infer the reason behind such an exponential growth of research on graphene since the last decade in the research community.
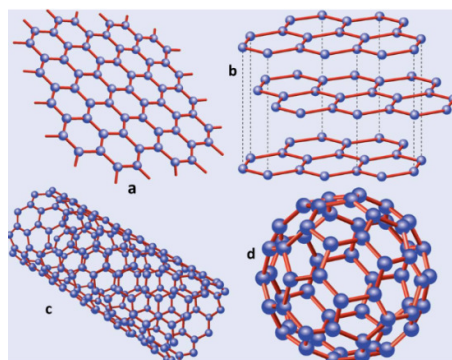

Fig. 1. (a) Graphene (b) Graphite (c) Carbon Nano tube (d) Fullerene. [Ref.64].

The reason behind such a detailed study of Graphene is due to its low manufacturing cost, which in turn leads to a much wider potential for applications in different electrical gadgets. The process through which it is synthesized can vary; of these techniques the most popular one such as mechanical exfoliation of highly oriented pyrolytic graphite (HOPG) [1, 8-13], reduction of graphene oxide sheets [15] chemical vapour deposition (CVD) [16-17], and thermal decomposition of silicon carbide [18]. Graphene coupled with polymer [19,20], inorganic surfaces [21,22], organic solvent [23], metal particles [24,25], biomaterials [26-28] and carbon nanotubes (CNTs) [29,30] are with great amount of success fabricated and are being rigorously observed in modern mechanical objects such as transparent conductors [29,31], batteries [32,33], supercapacitors [11,34], fuel cells [24], sensing platforms [35,36]. Despite having leaped forward in such a fashion in the field of research, graphene based composites are far behind from their large scale application because of the tiny sizes of the nanostructures and lack of their basic structure information. Therefore the study of the fabrication and characterization of graphene based materials is a big challenge for the researchers nowadays. These shortcomings can be overcome by using Computer modelling and simulation (CMS).

2. Study of Graphene through DFT

Computer modelling and simulation (CMS) is the best tool in explaining the structure, properties and other queries regarding graphene based composites by unveiling the new ways of

designing graphene based structure in complementary with the experiment [37]. CMS has been studied in great detail ranging from microscopic level to that of those that are clearly visible and can be witnessed through the naked eye. Recently, driven by the advances in high performance computational resources together with development of more efficient numerical algorithms has proven CMS to carry out the investigation on structural transformations of a defined material system as well as the interacting processes between different materials [38].
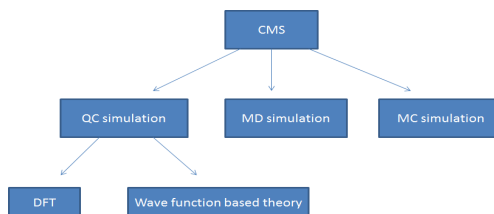

Fig. 2. Types of simulations applied for theoretical study of graphene.

Quantum chemistry method usually named as QC method of simulation, based on quantum mechanics, applies computational solution of the noble electronic Schrodinger equation (given by equation 1) for a typical simulation methodology [39].

$$\hat{H}\Psi = E\Psi \tag{1}$$

where $\hat{H}$ stands for the Hamiltonian operator given as

$$\hat{H} = \frac{-1}{2}\sum_{i=1}^{N}\nabla_i^2 - \frac{1}{2}\sum_{A=1}^{M}\frac{1}{M_A}\nabla_i^2 - \sum_{i=1}^{N}\sum_{A=1}^{M}\frac{Z_A}{r_{iA}} + \sum_{i=1}^{N}\sum_{j>i}^{N}\frac{1}{r_{ij}} + \sum_{A=1}^{M}\sum_{B>A}^{M}\frac{Z_A Z_B}{R_{AB}} \tag{2}$$

Ψ and E are the wave function and energy of the system, respectively. The first two terms describe the kinetic energy of the electrons and nuclei. The other three terms represent the attractive electrostatic interaction between the nuclei and the electrons and repulsive potential due to the electron-electron and nucleus-nucleus interactions.

Two highly productive approaches namely wave function based approach and density functional theory (DFT) have been widely applied to find the solution to the time independent Schrodinger equation. Born-Oppenheimer approximation assumes nucleus to move much slower than electrons giving its kinetic energy to be zero and potential energy to be constant in the Hamiltonian. The solution of the Schrodinger equation with the reduced Hamiltonian gives the electronic wave function and energy. For a system of N electrons and given nuclear potential V_{ext}, the variational principle defines a procedure to determine the ground-state wave function , the ground-state energy E_0 [N; V_{ext}], and other properties of interest. The ground state wave function and energy may be found by searching all possible wave functions for the one that minimises the total energy. The Hartree-Fock approximation is the method whereby the orthogonal orbitals are found that minimize the energy for this determinantal form of:

$$E_{HF} = min_{(\Psi \to N)}[\Psi_{HF}] \tag{3}$$

The question that arises is – "*Is it necessary to solve the Schrödinger equation and determine the 3N dimensional wave function in order to compute the ground state energy?*"

The first Hohenberg-Kohn theorem demonstrates that the electron density uniquely determines the Hamiltonian operator and thus all the properties of the system. The second theorem rephrases the variational principle that the ground state energy of the system, delivers the lowest energy if and only if the input density is the true ground state density. Determining the exchange correlation potential in Kohn Sham equations will lead to the exact energy of the system.

DFT study is the only method available to provide information like band structure, density of state (DOS) and so on. A keen literature survey [40-52] yielded that DFT plays an irreplaceable role in analyzing the nature and nanostructure of graphene.

3. Potential doping in graphene

Graphene along with extraordinary properties also exhibits a linear dispersing band at the K point of its Brillouin zone, named as the Dirac cone (E_D). On approaching E_D, the density of states (DOS) of the graphene, becomes linear and vanish away. However, as graphene is a zero band gap material, the formation of a small band gap is required for accurate function, whenever this material is used in the electronic industry. The nil band gap in graphene has troubled the effective application of graphene for semiconducting devices. These devices fail to show any 'off' state. Hence, the creation of a band gap is very critical issue for future applications of graphene in semiconducting devices.

Many experimental and theoretical techniques have been employed for the creation of band gap in graphene. Most famous of them are chemical doping [44] and adsorption [45]. Chemical doping, is one of the efficient way to modify the electronic properties, has been widely used in semiconductor industries. In order to have a perfect dopant for graphene, the element must have a matching lattice constant with that of graphene (1.4252 Å). It is important to note that the dopant should replace the carbon atom without disturbing the honey comb lattice of pure graphene also known as pristine. Doping on graphene sheet is found to improve its magnetic, optical, electrical, physicochemical and structural properties [46–52].

In the present article, we report some of the influence able study of doping on pristine (pure graphene). Opening of band gap of pristine due to principal doping has been focused in the discussion. Density Functional Theory (DFT) provides a variety of codes and packages for investigation and calculation of band gap of pure and doped graphene. It includes Quantum Espresso, VASP, SIESTA, Dmol3 and WEIN2K etc., using the appropriate approximation methods such as Local Density Approximation (LDA), Generalized Gradient Approximation (GGA). We have discussed only those dopants that have tailored to create an energy band gap in graphene.

3.1. Band gap opening by nitrogen and boron doping

Nitrogen and Boron are the most widely studied impurities in case of graphene. VASP code along with MedeA software package has been implemented for the study of band gap variation in pristine and doped graphene. Simulations were performed using GGA with Perdew–Burke–Ernzerhof (PBE) exchange and correlation. The hexagonal structure of pristine was being developed and N and B atoms were substituted by C for preparing doped graphene structure. Co-doping of these elements is the most favourable than other co-doping configuration. The concentration of doping elements had varied up to 18.75 % and in case of co doping the concentrations varied up to 31.25 %.

The electronic properties of these configurations can be evaluated from the DOS plot. Most important of them is the energy band gap value. DOS plots in figure 3 shows the pristine exhibits zero band gap value while opening of band gap has been observed with the addition of dopants to the pure structure. Moreover, band gap values are sensitive to the variation in the doping concentrations.

It is clear from figure 3a that pristine shows zero band gap value while in figure 3b Nitrogen doped graphene (NG) system shows band gap energy value below Fermi energy (E_f). In figure 3c Boron doped graphene (BG) system shows the value above E_f. Fermi energy level shifts towards conduction band in an n-type semiconductor while it shifts towards valence band in a p-type semiconductor. Hence, it has been shown that Nitrogen doped graphene is a P type semiconductor while Boron doped shows N type conductivity. A clear band gap is observed around the E_f by 25% of NBG system. This is due to the isoelectronic nature of N-B pair co-doping. It is quite evident that with respect to N and B substitution, N-B pair doping opens the band gap in graphene.
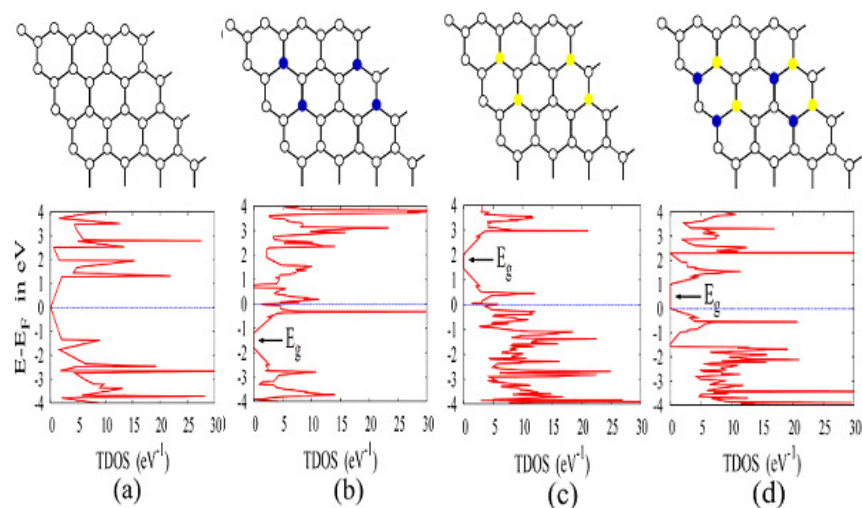
Fig. 3. Band structure of (a) pristine (b) Nitrogen doped graphene (c) Boron doped graphene
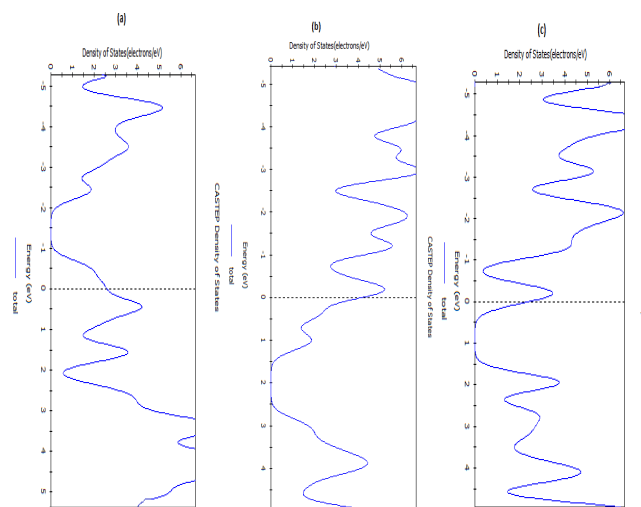*(d) Nitrogen Boron Co-doped graphene. Blue dotted line represents the Fermi level Ef. (Ref. 53).*

Fig. 4. DOS plots of (a) Nitrogen doped graphene (b) Boron doped graphene
(c) Nitrogen Boron Co-doped graphene.

Table 1 also shows a comparison of the band gap values calculated for such configurations.

Table 1. Band gap of extrinsic graphene.

Material	Ref [53]	Our study
BG	0.7eV	0.379 eV
NG	0.6eV	0.386 eV
NBG	1eV	0.712 eV

In Fig. 5, the sensitivity of graphene to band gap opening has been shown in relation to the doping concentration. As the doping concentration is increased, energy band gap originated in the configuration. It can be interpreted from the graph in Fig. 5 that the band gap varies linearly with the doping concentration and it is irrespective of the type of the foreign atoms added to it [53]. It is interesting to note that up to 16% of the doping concentration of N and B in NG and BG systems, respectively, the value of E_g does not depend on doping type. In comparison to NG and BG system, a slightly less magnitude of E_g has been noticed for NBG systems.
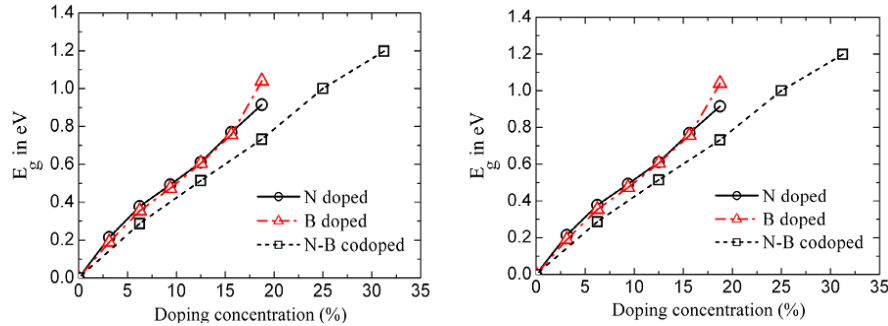

Fig. 5. Band gap opening versus doping concentration.[Ref. 53]. Reprinted figure with permission from [53] Copyright 2014 by the Elsevier Publishing Group

Rani *et al.* [54] also reports doping of Boron and Nitrogen on pristine having doping concentration in the varying parameters. PBE-GGA functional was adopted under the VASP software code. Doping results in the decrease of C-C bond length due to large covalent radius of Boron. As a result, bond length expanded to 1.48 Å. Due to electron deficient character of boron, Fermi level shifts significantly to 0.7 eV below the Dirac point resulting into p-type nature. Breaking of two graphene sub lattices occur which causes a band gap of 0.14 eV around the Dirac point. Therefore, as the concentration of Boron atom is increased, it increases the lattice disorder that leads to the increase in the band gap values.

Similar effects have been observed using Nitrogen as the foreign species. The bond length of three N-C bonds formed is 1.40 Å and there is almost no distortion in the planar structure of graphene. But due to electron rich character of the resulting structure, the Fermi level shifts by 0.7eV above the Dirac point. In this study, almost same behaviour and trends have been shown by both Boron and nitrogen. A band gap of 0.14 eV has been produced in pristine via Boron and Nitrogen doping [54].

Zhang *et al.* [55] also reports Nitrogen doping onto pure graphene lattice. In this research, The DFT program DMol$_3$ in Materials Studio (Accelrys, San Diego, CA) was used to investigate the interactions between the doped or intrinsic graphene. After drawing an optimized intrinsic graphene structure, one carbon atom was replaced by Nitrogen atom. According to the calculations the bond length of carbon-carbon bond was 1.4252 Å while that of carbon nitrogen bond was 1.4145 Å. After replacement of one carbon atom by nitrogen leaves the carbon atom positively charged. These investigations prove nitrogen to be an electron rich dopant [55].

Méndez *et al.* [46] reports that the addition of holes and electrons in pristine are mainly by boron and nitrogen doping. This alteration in the electronic properties by controlled doping in pristine plays a vital role in the advancement of field effect transistor and p-n junctions. In general, STM image simulation is carried out under the Tersoff–Hamann [56] approximation is good enough for screening possible atomic configurations of the dopant atoms. The STM images can be generated by using the shaded region of density of states (DOS) plot. These images depict the changes in the density due to single, double and triple substitutions shown in figure 6 [46].
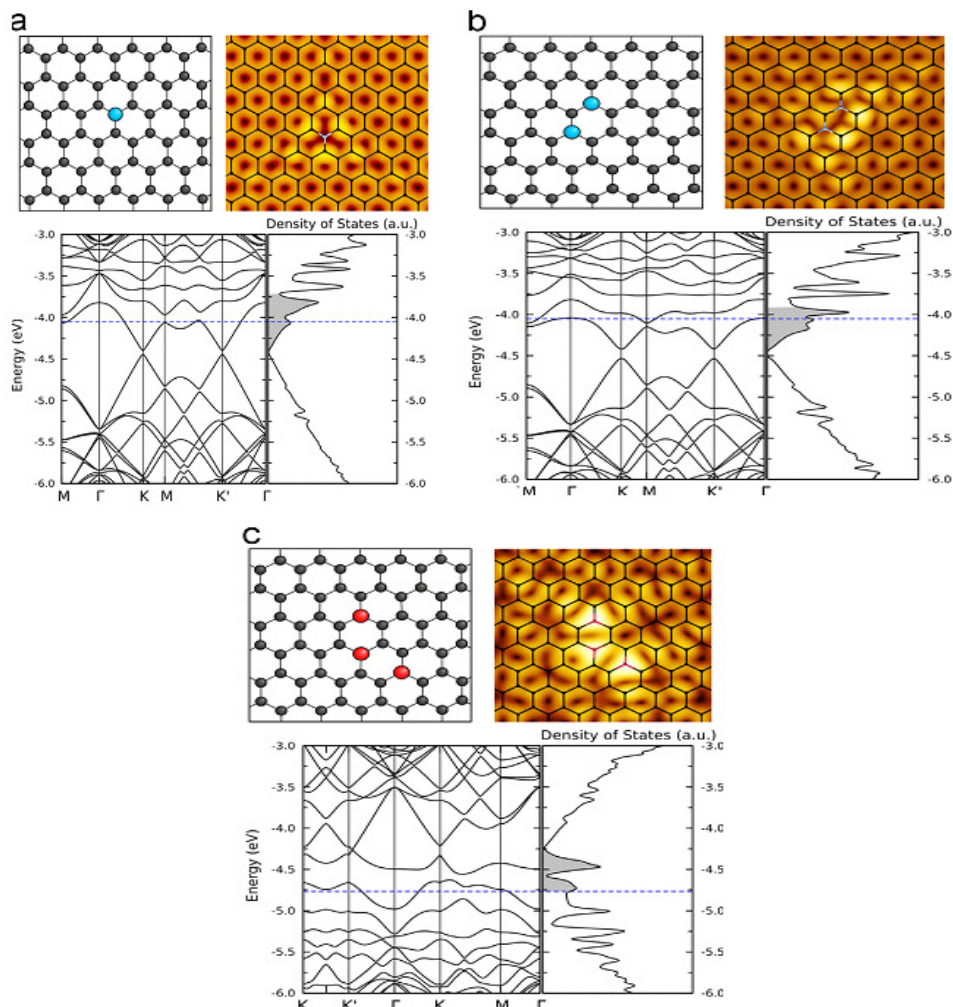
Fig. 6. The modelled structure, STM image, band structure and DOS plot of (a) single substitutional Nitrogen doping (b) double substitutional Nitrogen doping (c) triple substitutional Boron doping, Blue dotted line represents the Fermi level E_f. Reprinted figure with permission from [46] Copyright 2013 by the Elsevier Publishing Group.

Hexagonal boron nitride (h-BN) has been studied as a dopant on pristine with different concentrations. The calculations are carried out using DFT with the generalized gradient approximation (GGA) and projector augmented wave (PAW) method, as implemented in the VASP code [57]. The BN concentration in the study was 1%, 2% and 3% corresponding to one BN, two BN and three BN pairs, respectively. The band Gap of one BN pair embedded graphene opens up to (0.616eV), 2BN pair increase upto(0.386eV), 3BN pair sharply increases the band gap up to (1.457ev),when replace by (2,4,6) carbon atoms. Embedded BN pairs in graphene break the inversion symmetry, which can result in the opening up of bandgap in graphene. The P_z orbitals of B and N hybridize with P_z orbital of C, which break the reversal symmetry b/w π and π^* orbital of C. Fermi level keeps lying in the centre of forbidden energy band, an intrinsic semiconducting band structure characteristic which shows that BN doped graphene has potential application in electronic devices. Not surprising, one BN pair has 8 valance electrons, the same as two carbon atoms, hence no extra electrons holes are injected in BN embedded graphene, and no driving force to shift Fermi level.
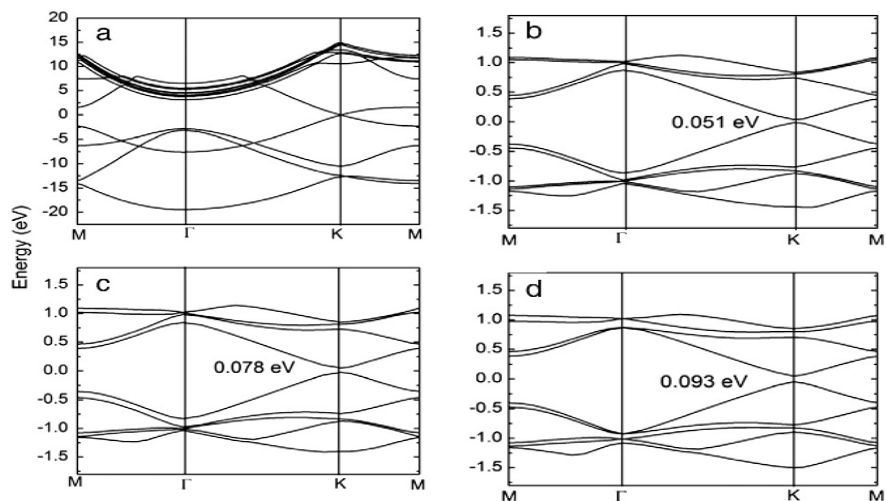
Fig. 7. (a) pristine (b) one BN pair doped graphene (c) two BN pair doped graphene (d) three BN pair doped graphene. Reprinted figure with permission from [57] Copyright 2014 by the Elsevier B.V. Publishing Group.

Fig. 8 interprets the band gap calculations according to our study for the pure Graphene and with different doping of BN pairs in the pure structure.
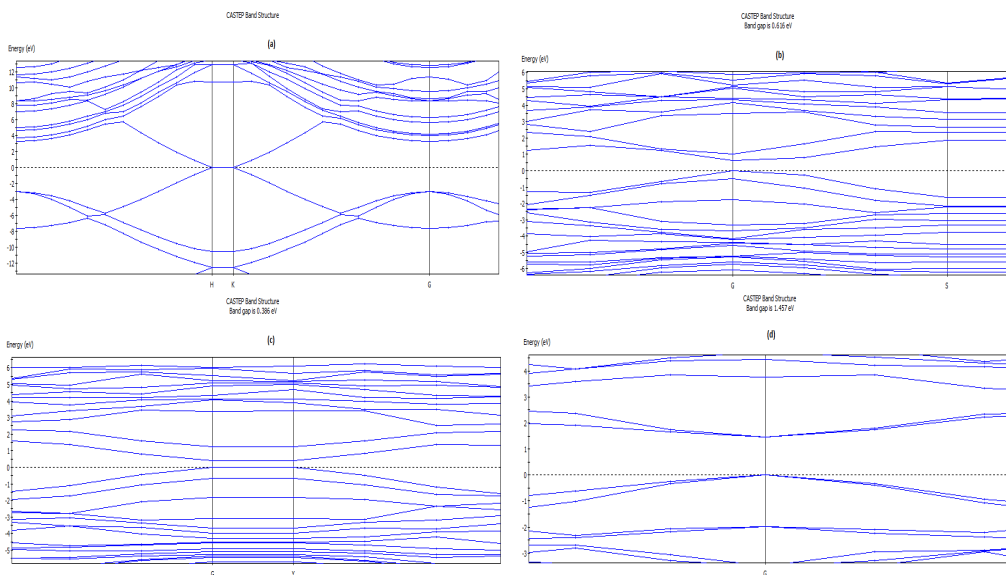

Fig. 8. Our calculation (a) pristine (0 eV) (b) one BN pair doped graphene (0.616 eV) (c) two BN pair doped graphene (0.386 eV) (d) three BN pair doped graphene (1.467 eV).

Table 2 shows the bond lengths of the dopants with the carbon atom in the lattice that determines the stability of the doped lattice structure. The values are close to the carbon-carbon bond lengths in pristine.

Table 2. Relative bond lengths of carbon forming with itself and the dopants.

d_{C-C}	d_{C-N}	d_{C-B}	d_{B-N}
1.426 Å [57]	1.4145 Å [55]	1.4512 Å [54]	1.461 Å [57]

3.2. Si doped graphene

The complete explanation of the band gap of a material requires a two particle theory, hence DFT is not enough to describe this property by itself after all it is a one particle theory. Bethe Salpeter equation (BSE) or GW must be used for solids along with codes like WEIN2K [58-59]. In order to save time and memory, the effect of silicon on the electronic properties of graphene was studied by performing G_0W_0 and TB-mBJ calculations [60]. Calculations revealed the band gap of graphene is nearly zero, this result shows that the gapless characteristic observed in graphene is an intrinsic property. Silicon has a larger atomic radius than carbon, therefore due to intense interaction there will be a strong repulsion force between Si and C. This results in the opening of the band-gap and hybridization between the p orbital for both Si and C, whereas the σ band remains unchanged contrary to π band. Same trend, as in [53, 54], has been followed: increase in concentration increases the band gap opening except at lower concentration of Si for which here is no change in the electronic behaviour [60].
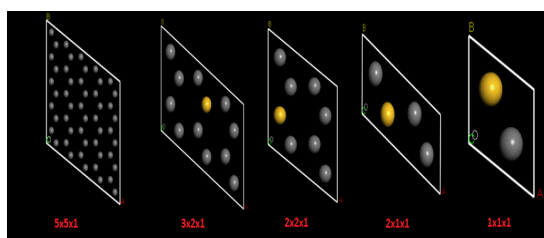

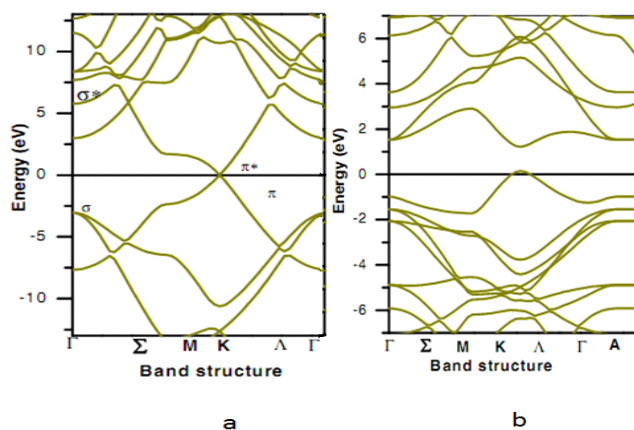*Fig. 9. The supercell of pure and doped graphene structure.*

Fig. 10. Energy band gap structure (a) pristine (b) at 12.5 % concentration of Si doping.
Reprinted figure with permission from [60] Copyright 2015 by the Elsevier Publishing Group.
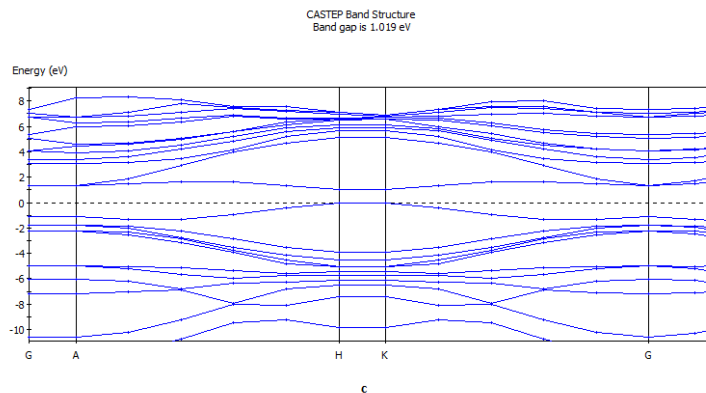
Fig. 11. Band gap at 12.5 % concentration of Si doping.

Fig. 10 shows a band gap opening of 1.4 eV at 12.5 % concentration of Si doping. But in our calculation the band gap opening is 1.019 eV at 12.5%. Furthermore the table 3 shows the band gap values corresponding to the Si concentration.

Table 3. Band gap values of graphene as a function of Silicon concentration.

Concentration of Silicon	0%	8.33%	12.50 %	25%	50%
Band gap of graphene (eV)	0	1.022	1.357	1.955	2.51
This work (eV)	0	0.896	1.019eV	1.687eV	2.72eV

It has also been reported that silicon doping increases the optical conductivity of graphene in visible region and it allows the graphene to be used in photovoltaic cells [60].

Doping has been extended to the second row atoms of the lattice of monolayer pristine and then characterized for results. DFT calculations, using the PBE and LDA functional, have been implemented in SIESTA to study second row atom doping in graphene [61]. Silicon has the lowest formation energy. However, it is not effective enough for opening a band gap in the band structure of graphene. The reduction of band gap for 6x6 models are observed for silicon, when the level of doping is further decreased the band gap is increased again. Si is the least effective second row atom to open a band gap in graphene, inducing very few changes on its band structure, probably because it has the same no of valance electrons, and thus the occupation of the bands may not be changed. In the case of 4x4 model the system is semi metallic, the π^{*} band slightly crosses the Fermi level, and for the other models the system is semiconductor (0.57eV-1.90eV). Table 4 shows the values of band gap obtained for Si doped on monolayer graphene [61].

Table 4. The band gap values of monolayer graphene with Silicon for different cell dimensions.

Graphene super cell dimensions	Energy Band gap (in eV) [61]	This work
4×4	0.02	1.22
5×5	0.06	1.90
6×6	0.08	0.57
7×7	0.02	0.59
8×8	0.01	1.27

3.3. Aluminum (Al) doped Graphene

Al doped graphene has one of the unstable configuration because of its larger formation energy which is around 10 eV. But it is worth attention because it gives metallic behaviour to graphene. Most important thing to notice is that addition of Al as a dopant does not produce any band gap in pristine. Al has the largest formation energy and thus forms the weakest bond with carbon [60-62].

4. Experimental studies on doped Graphene

There is wide diversity in the methods used for the synthesis of pure and doped graphene currently classified as *in situ* approaches and post-treatment approaches. Wang *et al*. [63] provided a detail section on the experimental techniques followed for preparing doped graphene via different approaches.
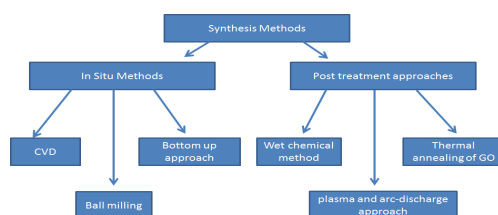

Fig. 12. Different synthesis techniques for pure and doped graphene.

Table 5 describes the summary of all the experimental studies for the synthesis of graphene and doped graphene using different precursors. Among all these techniques, CVD technique is the most effective and widely studied but it is very expensive as compared to other approaches. Moreover, all methods exhibit a low yield ratio which makes graphene difficult to be handled and tuned up.

As far as the band structure is concerned, there is no direct experimental technique to find out the value for a given sample. Furthermore, no experimental evidence has been provided for the impact on the band gap via doping whereas researchers are using the data evaluated from the simulations in their experimental studies. A hit and trial method is followed for implementing intrinsic and extrinsic graphene for various applications. Results and performance of the device fabricated, using graphene and its products, decide whether graphene is a good option for large scale application. It should be noted that the same dopants are used experimentally that have been tested via simulations.

Table 5. Summary of graphene doping techniques [63].

Methods	Precursors	Doping
CVD	H_3BO_3 + polystyrene	4.3 at% B
	Phenylboronic acid	1.5 at% B
	CH_4 +H_3NBH_3	10–90 at% BN
	CH_4 +NH_3	8.9 at% N
	Sulfur in hexane	<0.6 at% S
	Iodine + camphor	3.1 at% I
	Pyrimidine + thiophene	5.7 N, 2.0 S at%
Ball milling	Pristine graphite (PG) + N_2	14.8 wt% N
	PG + sulfur powder	4.94 at% S
	PG + Cl_2/Br_2	5.85 Cl/2.78 Br at%
Bottom-up synthesis	CCl_4 + K + BBr_3	2.56 at% B
	Li_3N + CCl_4	4.5–16.4 at% N
	Pentachloropyridine + K	3.0 at% N
Thermal annealing	GO + BCl_3	0.88 at% B
	GO + NH_3	8 at% N
	GO + melamine/PANI/PPy	2–18 at% N
	GO + ionic liquid	22.1 N/1.16 P at%
	GO + H_2S	1.2–1.7 at% S
	GO + DDS + DDSe	0.19 S, 0.05 Se at%
	Graphite oxide + Cl_2/Br_2	5.9 Cl/9.93 Br at%
Wet chemical method	GO + hydrazine	4.5 at% N
	GO + urea	10.13 at% N
	GO + NH_4SCN	18.4 N, 12.3 S at%
	GO + HF/HI	1.38 F/4.33 I wt%
	PG + Cl_2/Br_2	21 Cl/ 4 Br at%
Plasma	GO + N_2	2.51 at% N
	CVD graphene + Cl_2	45.3 at% Cl
Photo-chemistry	CVD graphene + Cl_2, xenon lamp irradiation	8 at% Cl
Arc-discharge	PG + NH_3	1 at% N
	PG + B/B_2H_6	3.1 at% B
	PG + graphite fluoride	10 wt% F

5. Conclusions

The structural and electronic properties of intrinsic and extrinsic graphene can be vividly described by DFT studies. It can be summarized that doping of different impurities significantly alters the electronic and optical properties of graphene Nano sheet especially in band structure. Doping pristine graphene opens up the band gap value in the geometry and it increases with the increase in the doping concentration in the material. Nitrogen and Boron substitution and pair doping in graphene shows that B and N open up a band gap up to (0.386eV) and (0.379eV),while co-doping of B-N create a band gap up to (0.712 eV), where as its pair doping shows that 1BN create band gap (0.616eV),2BN create(0.386eV),3BN create a sharp band gap up to(1.457eV) .The study of substitution doping and increased in the supercells models with the same doping concentration shows that the silicon induced a band gap of 1.019eV,where as Si doping on different super cells shows a band gap enhancement from 0.57eV at (6x6) model to 1.90eV at (5x5) model and change its nature from semi metal to semiconductor, while aluminium does not have any significant change in the band structure of pristine. Further investigations are likely to be rewarding, both in the context of experimental verification as well as for the further exploration of properties of doped graphene.

References

[1] K. S. Novoselov, A. K. Geim, S. V. Morozov, D. Jiang, Y. Zhang, S. V. Dubonos, A. A. Firsov, Science **306**(5696), 666 (2004).

[2] A. G. Marinopoulos, L. Reining, A. Rubio, V. Olevano, Physical Review B **69**(24), 245419 (2004).

[3] F. Bonaccorso, Z. Sun, T. Hasan, A. C. Ferrari, Nature photonics **4**(9), 611 (2010).

[4] L. A. Falkovsky, in Journal of Physics: Conference Series **129**(1), 012004 (2008).

[5] T. Eberlein, U. Bangert, R. R. Nair, R. Jones, M. Gass, A. L. Bleloch, P. R. Briddon, Physical Review B **77**(23), 233406 (2008).

[6] J. L. Cheng, C. Salazar, J. E. Sipe, Physical Review B **88**(4), 045438 (2013).

[7] M. Gmitra, S. Konschuh, C. Ertler, C. Ambrosch-Draxl, J. Fabian, Physical Review B **80**(23), 235431 (2009).

[8] K. S. Novoselov, Z. Jiang, Y. Zhang, S. V. Morozov, H. L. Stormer, U. Zeitler, A. K. Geim, Science **315**(5817), 1379 (2007).

[9] V. P. Gusynin, S. G. Sharapov, Physical Review Letters **95**(14), 146801 (2005).

[10] R. R. Nair, P. Blake, A. N. Grigorenko, K. S. Novoselov, T. J. Booth, T. Stauber, A. K. Geim, Science **320**(5881), 1308 (2008).

[11] M. D. Stoller, S. Park, Y. Zhu, J. An, R. S. Ruoff, Nano letters **8**(10), 3498 (2008).

[12] C. Lee, X. Wei, J. W. Kysar, J. Hone, Science **321**(5887), 385 (2008).

[13] S. Stankovich, D. A. Dikin, G. H. Dommett, K. M. Kohlhaas, E. J. Zimney, E. Stach, R. S. Ruoff, Nature **442**(7100), 282 (2006).

[14] A. K. Geim, K. S. Novoselov, Nature materials **6**(3), 183 (2007).

[15] S. Stankovich, D. A. Dikin, G. H. Dommett, K. M. Kohlhaas, E. J. Zimney, E. A. Stach, R. S. Ruoff, Nature **442**(7100), 282 (2006).

[16] A. Reina, X. Jia, J. Ho, D. Nezich, H. Son, V. Bulovic, J. Kong, Nano letters **9**(1), 30 (2008).

[17] R. John, A. Ashokreddy, C. Vijayan, T. Pradeep, Nanotechnology **22**(16), 165701 (2011).

[18] C. Berger, Z. Song, X. Li, X. Wu, N. Brown, C. Naud, E. H. Conrad, Science **312**(5777), 1191 (2006).

[19] T. Ramanathan, A. A. Abdala, S. Stankovich, D. A. Dikin, M. Herrera-Alonso, R. D. Piner, S. T. Nguyen, Nature nanotechnology **3**(6), 327 (2008).

[20] J. L. Vickery, A. J. Patil, S. Mann, Advanced Materials **21**(21), 2180 (2009).

[21] J. S. Moon, D. Curtis, M. Hu, D. Wong, C. McGuire, P. M. Campbell, C. Eddy, IEEE Electron Device Letters **30**(6), 650 (2009).

[22] Z. H. Ni, W. Chen, X. F. Fan, J. L. Kuo, T. Yu, A. T. S. Wee, Z. X. Shen, Physical Review B **77**(11), 115416 (2008).

[23] S. Villar-Rodil, J. I. Paredes, A. Martínez-Alonso, J. M. Tascón, Journal of Materials Chemistry **19**(22), 3591 (2009).

[24] C. Xu, X. Wang, J. Zhu, The Journal of Physical Chemistry C **112**(50), 19841 (2008).

[25] S. Y. Zhou, D. A. Siegel, A. V. Fedorov, A. Lanzara, Physical review letters **101**(8), 086402 (2008).

[26] W. Lv, M. Guo, M. H. Liang, F. M. Jin, L. Cui, L. Zhi, O. H. Yang, Journal of Materials Chemistry **20**(32), 6668 (2010).

[27] N. Mohanty, V. Berry, Nano letters **8**(12), 4469 (2008).

[28] J. Liu, S. Fu, B. Yuan, Y. Li, Z. Deng, Journal of the American Chemical Society **132**(21), 7279 (2010).

[29] J. Liu, S. Fu, B. Yuan, Y. Li, Z. Deng, Journal of the American Chemical Society **132**(21), 7279 (2010).

[30] Y. K. Kim, D. H. Min, Langmuir **25**(19), 11302 (2009).

[31] S. Watcharotone, D. A. Dikin, S. Stankovich, R. Piner, I. Jung, G. H. Dommett, S. T. Nguyen, Nano letters **7**(7), 1888 (2007).

[32] T. Yoon, M. Cho, Y. W. Suh, E. S. Oh, J. K. Lee, Journal of nanoscience and nanotechnology **11**(11), 10193 (2011).

[33] Z. Du, X. Yin, M. Zhang, Q. Hao, Y. Wang, T. Wang, Materials Letters **64**(19), 2076 (2010).

[34] Y. Wang, Z. Shi, Y. Huang, Y. Ma, C. Wang, M. Chen, Y. Chen, The Journal of Physical Chemistry C **113**(30), 13103 (2009).

[35] J. Balapanuru, J. X.Yang, S. Xiao, Q. Bao, M. Jahan, L. Polavarapu, K. P. Loh, Angewandte Chemie **122**(37), 6699 (2010).

[36] P. K. Ang, W. Chen, A. T. S. Wee, K. P. Loh, Journal of the American Chemical Society **130**(44), 14392 (2008).

[37] A. Du, S. C. Smith, The journal of physical chemistry letters **2**(2), 73 (2010).

[38] T. Zhang, Q. Xue, S. Zhang, M. Dong, Nano Today **7**(3), 180 (2012).

[39] D. R. Hartree, in Mathematical Proceedings of the Cambridge Philosophical Society **24**(01), 89 (1928).

[40] R. A. Friesner, Proceedings of the National Academy of Sciences of the United States of America **102**(19), 6648 (2005).

[41] V. Fock, Zeitschrift für Physik **61**(1-2), 126 (1930).

[42] P. Hohenberg, W. Kohn, Phys. Rev. B **136**, 864 (1964).

[43] M. Levy, Proc. Natl. Acad. Sci. **76**(12), 6062 (1979).

[44] X. Fan, Z. Shen, A. Q. Liu, J. L. Kuo, Nanoscale **4**(6), 2157 (2012).

[45] F. Yavari, C. Kritzinger, C. Gaire, L. Song, H. Gulapalli, T. Borca-Tasciuc, N. Koratkar, Small **6**(22), 2535 (2010).

[46] A. R. Botello-Méndez, A. Lherbier, J. C. Charlier, Solid State Communications **175**, 90 (2013).

[47] S. T. Skowron, I. V. Lebedeva, A. M. Popov, E. Bichoutskaia, Chemical Society Reviews **44**(10), 3143 (2015).

[48] X. Wang, G. Sun, P. Routh, D. H. Kim, W. Huang, P. Chen, Chemical Society Reviews **43**(20), 7067 (2014).

[49] Y. Ito, C. Christodoulou, M. V. Nardi, N. Koch, M. Kläui, H. Sachdev, K. Müllen, Journal of the American Chemical Society **137**(24), 7678 (2015).

[50] N. Chen, X. Huang, L. Qu, Physical Chemistry Chemical Physics **17**(48), 32077 (2015).

[51] L. Vicarelli, S. J. Heerema, C. Dekker, H. W. Zandbergen, ACS nano **9**(4), 3428 (2015).

[52] X. Wang, G. Shi, Physical Chemistry Chemical Physics **17**(43), 28484 (2015).

[53] P. Nath, S. Chowdhury, D. Sanyal, D. Jana, Carbon **73**, 275 (2014).

[54] P. Rani, V. K. Jindal, RSC Advances **3**(3), 802 (2013).

[55] H. P. Zhang, X. G. Luo, X. Y. Lin, X. Lu, Y. Leng, International journal of hydrogen energy **38**(33), 14269 (2013).

[56] J. Tersoff, D. R. Hamann, Physical review letters **50**(25), 1998 (1983).

[57] Z. G. Yu, Y. W. Zhang, Diamond and Related Materials **54**, 103 (2015).

[58] F. Aryasetiawan, O. Gunnarsson, Reports on Progress in Physics **61**(3), 237 (1998).

[59] G. Baym, L. P. Kadanoff, Physical Review **124**(2), 287 (1961).

[60] M. Houmad, H. Zaari, A. Benyoussef, A. El Kenz, H. Ez-Zahraouy, Carbon **94**, 1021 (2015).

[61] P. A. Denis, Chemical Physics Letters **492**(4), 251 (2010).

[62] J. Dai, J. Yuan, P. Giannozzi, Applied Physics Letters **95**(23), 232105 (2009).

[63] X. Wang, G. Sun, P. Routh, D. H. Kim, W. Huang, P. Chen, Chemical Society Reviews **43**(20), 7067 (2014).